



Article

# High-Pressure FDM 3D Printing in Nitrogen [Inert Gas] and Improved Mechanical Performance of Printed Components

Yousuf Pasha Shaik <sup>\*</sup>, Jens Schuster and Naresh Kumar Naidu

Department of Applied Logistics and Polymer Sciences, University of Applied Sciences Kaiserslautern, 66953 Pirmasens, Germany

\* Correspondence: [yousuf.shaik@hs-kl.de](mailto:yousuf.shaik@hs-kl.de) or [yousufpashashaik@gmail.com](mailto:yousufpashashaik@gmail.com)

**Abstract:** Fundamentally, the mechanical characteristics of 3D-printed polymeric objects are determined by their fabrication circumstances. In contrast to traditional polymer processing processes, additive manufacturing requires no pressure during layer consolidation. This study looks at how a high-pressure autoclave chamber without oxygen affects layer consolidation throughout the fused deposition modelling process, as well as the mechanical qualities of the products. To attain high strength qualities for 3D-printed components such as injection-molded specimens, an experimental setup consisting of a 3D printer incorporated within a bespoke autoclave was designed. The autoclave can withstand pressures of up to 135 bar and temperatures of up to 185 °C. PLA 3D printing was carried out in the autoclave at two different pressures in compressed air and nitrogen atmospheres: 0 bar and 5 bar. Furthermore, injection molding was done using the same PLA material. Tensile, flexural, and Charpy tests were carried out on samples that were 3D printed and injection molded. In nitrogen, oxidation of the environment was prevented by autoclave preheating before printing, and autoclave pressure during printing considerably promotes layer consolidation. This imparted mechanical strength on the 3D-printed items, which are virtually as strong as injection-molded components.

**Keywords:** autoclave; 3D printing; mechanical properties; additive manufacturing; layer consolidations; nitrogen atmosphere



**Citation:** Shaik, Y.P.; Schuster, J.; Naidu, N.K. High-Pressure FDM 3D Printing in Nitrogen [Inert Gas] and Improved Mechanical Performance of Printed Components. *J. Compos. Sci.* **2023**, *7*, 153. <https://doi.org/10.3390/jcs7040153>

Academic Editor: Francesco Tornabene

Received: 2 March 2023

Revised: 21 March 2023

Accepted: 4 April 2023

Published: 10 April 2023



**Copyright:** © 2023 by the authors. Licensee MDPI, Basel, Switzerland. This article is an open access article distributed under the terms and conditions of the Creative Commons Attribution (CC BY) license (<https://creativecommons.org/licenses/by/4.0/>).

## 1. Introduction

Using CAD models, additive manufacturing (AM) technology promises to fabricate complex and multifunctional components and products in a single step [1]. It is defined as “the method of layering materials like polymer, metal, concrete, ceramics, or rubber in consecutive layers on top of one other.” [2].

Rapid prototyping and additive manufacturing, sometimes referred to as 3D printing, are not new concepts. Stereolithography (SL), the first 3D-printing method, was created in 1984 by Charles W. Hull of the 3D Systems Corporation, and was exceedingly costly. [3]. Initially, designers and architects were the main users of fast prototyping because of its capacity to produce working prototypes. Afterwards, a great deal of study was done, and incredible progress was made. As a result, several other additive manufacturing (AM) processes were created, including fused deposition modeling (FDM), materials jetting, inkjet printing, powder bed fusion, and others.

These developments in AM have lowered prices, productivity, and waste, while boosting printing quality, accessibility, sustainability, and usability [3].

These developments have boosted its applicability in automotive, aviation, medical, construction, and other areas [4]. Cheap cost and practicality give FDM a leading position in a wide range of sectors, from small-scale to large-scale, and may also be controlled by people.

FDM is a method in which a circular cross-sectional filament of a preset diameter is created to push into the hot-end through a feeder at a defined speed, and melted material

exits from the nozzle attached to the hot-end, following a prescribed route to construct a specimen layer by layer. The route and process parameters can be provided and controlled via software known as slicer [5]. (Printing patterns, infill density, infill angle, nozzle temperature, printing speed, and so on.)

FDM is a cost-effective approach to swiftly generate prototypes and functional components, in addition to affordable equipment and straightforward technological procedures, as shown in Figure 1. FDM parts, on the other hand, have drawbacks in terms of their mechanical properties. Among all 3D-printing technologies, these parts have the lowest dimensional accuracy and resolution [6]. Moreover, the visible layer lines in the sections of an FDM model require removal by post-processing in order to provide a smooth, flat surface and less uniform behavior. While FDM fast prototyping has several uses, anisotropic mechanical qualities make it useless for producing structural elements [7]. Its usage is restricted in many applications because of this drawback.

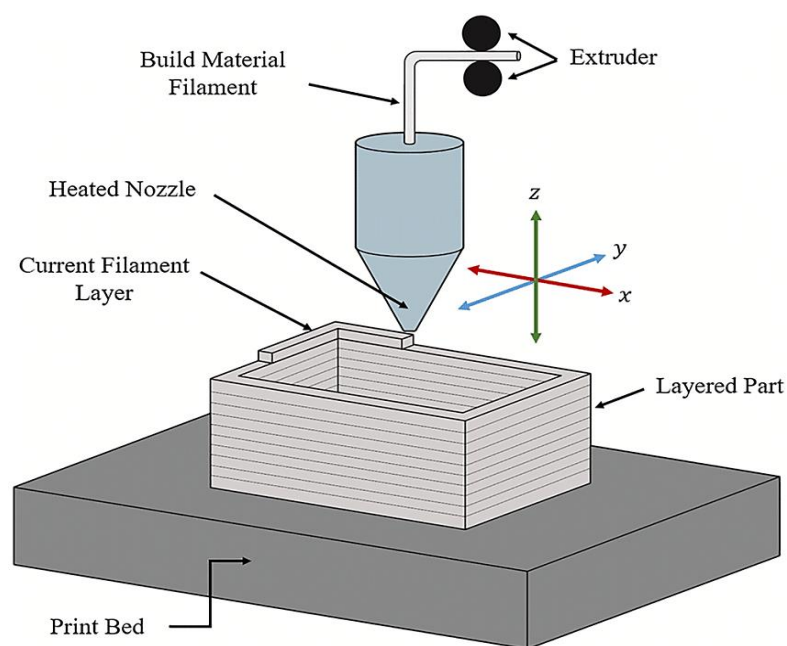


**Figure 1.** Overview of the FDM process.

The mechanical characteristics of products manufactured using 3D printing are now the subject of several research investigations. Examples of important printing parameters that are utilized to enhance their qualities include infill density, infill pattern, extrusion temperature, nozzle diameter, layer thickness, raster array, and others. Moreover, when natural and synthetic fibers (small fibers or long continuous fibers) are used to reinforce 3D-printed objects, the results are unsatisfactory [5].

A typical FDM printer's tensile strength increased by 30% when placed in the nitrogen environment, according to studies, when printing components [8].

Another study found that 3D-printed pieces that had been heated up had better interlayer adhesion and less internal stress [9,10]. The constraints of an annealing process, on the other hand, stem from the fact that some polymers are temperature sensitive, and may experience warping or shrinking due to heat.

The post-treatment procedure for better compaction of polymer material produced by FDM was the topic of one of our earlier investigations.

Four distinct designs with differing infill densities were mechanically tested before being put in a high-pressure autoclave, with the best pattern being used for post-treatment. The 3D-printed PLA samples were put in a special autoclave and subjected to 50 bar of pressure for 10 h at a temperature below the glass transition range.

Samples pick up moisture from the hot, compressed air in the autoclave, which leads to the development of internal crystallization. A bigger grain structure has been produced by rearranging the grain structure. Strength and modulus growth were assisted by this. Its mechanical characteristics were improved by around 20% as a consequence of the combined effects of pressure and temperature, which reduced internal tensions and enhanced grain structure [11].

Another study used an autoclave to carry out 3D printing at temperatures below or equivalent to the glass transition temperature. At this temperature, pressurization helped to prevent warping, improve layer consolidation, and remove any voids. A much greater tensile modulus was achieved. However, specimen strength is mostly unaffected by flexural and impact strength. Weight alterations were also brought on by internal molecular rearrangement [6].

By employing the atomization process to introduce cellulose nanocrystals (CNCs) between neighboring polymer layers, it is also possible to enhance the mechanical characteristics of 3D-printed polymer objects. The CNCs that are sprayed between printing layers serve as nano-stitches, enhancing the strength and adherence of the layers [12].

To enhance their mechanical characteristics, 3D-printed items can also be strengthened using additional materials or fibers. While these composite filaments are more costly than straight PLA or straight PETG, they are utilized in specialized applications with high loading capabilities, similar to PLA and PETG with carbon fibers [13].

The strength of FDM products is influenced by processing factors such as nozzle material, nozzle diameter, extrusion temperature, bed temperature, input materials (whether fresh or recycled), and fan speed, among others. The printing instructions have an effect as well. Poor mechanical qualities might be attributed to insufficient adhesion between the deposited layer and the incoming extruding material during printing. As it depends on extruding and cooling hot material, this might be due to the temperature differential between already-deposited films and the incoming layers [14].

Another research discovered that 3D-printed FDM components have more contained voids than injection-molded ones due to pressure throughout the process and strong dimensional control [15]. These voids combine with mechanical strength. Pressure is crucial in influencing the isotropic behavior of components. Voids can be controlled by reducing layer thickness and adjusting infill density. In such circumstances, micro voids are present but cannot be eradicated.

The majority of research works were done to increase the surface quality of 3D-printed items. Thermal treatment, chemical solution spraying, and coating of 3D-printed objects result in more isotopically behavior, which minimizes voids and enhances layer consolidation, resulting in enhanced mechanical qualities.

Nevertheless, no scientific or mechanical setup had been devised to incorporate a 3D printer within a chamber while maintaining pressure and temperature control throughout the whole process. In practically all techniques for increasing the mechanical characteristics of 3D-polymer-printed objects, pressure and temperature are the most significant and crucial elements.

Based on prior research findings, this study intends to attain high strength attributes in 3D printing similar to the conventional approach (injection molding). This can be achieved by enhancing the bonding quality of layer interfaces and preventing vacancies.

The purpose of this research is to 3D-print specimens in an autoclave with the same infill density and process parameters at 0 bar, 5-bar compressed air, and 5-bar nitrogen gas atmosphere in the transverse, longitudinal direction to the hot-end nozzle, and investigate the effect of inert gas environment on layer consolidations.

Tensile, flexural, and Charpy tests were performed on all specimens, and properties such as yield strength, yield strain, and Young's modulus, flexural, and impact strength were found. The results of the tests are compared to injection-molded specimens.

## 2. Materials and Methods

### 2.1. Material

This project made use of high-quality pure PLA (polylactic acid) filament from Herz GmbH in Germany. At EUR 25 for 1 kg, the filament is not excessively priced. Filaments are normally available in two diameters: 1.75 mm and 2.85 mm, although a 1.75 mm diameter was employed for this research [16].

PLA is a biodegradable polymer that biodegrades in industrial composting settings (in days or months). It is manufactured from renewable materials such as cornstarch or sugar cane. PLA filaments are expected to be employed in FDM because of their low melting point (180–220 °C), ability to support excellent surface prints, non-toxicity, good UV resistance, minimal moisture absorption, and simplicity of handling. In addition to its impact resistance, PLA outperforms other polymers including polyethylene (PE), polypropylene (PP), polyamide (PA), polyethylene terephthalate (PET), and polystyrene in terms of Young's modulus, tensile strength, and flexural strength (PS). It is utilized for quick prototyping because of these advantages [17]. The glass transition temperature of PLA is very low at 65 °C, which restricts its use in thermally demanding products. PLA is also hindered by its biodegradability.

### 2.2. Machines

#### 2.2.1. FDM 3D Printer

In this work, a Creality 2020 Ender-3, V2 model FDM 3D Printer, which is shown in Figure 2, was utilized. The mechanical axes for the extruder head and print bed are set up in the Cartesian XZ-Head order, with the extruder head moving along the X and Z axes and the print bed along the Y axis. The machine's overall weight is 7.8 kg, and its highest feasible dimensions are 220 × 220 × 250 mm (L\*BH\*) [18]. The maximum extruder temperature is 250 °C, the maximum bed temperature is 100 °C, and the maximum printing speed is 180 mm/s.

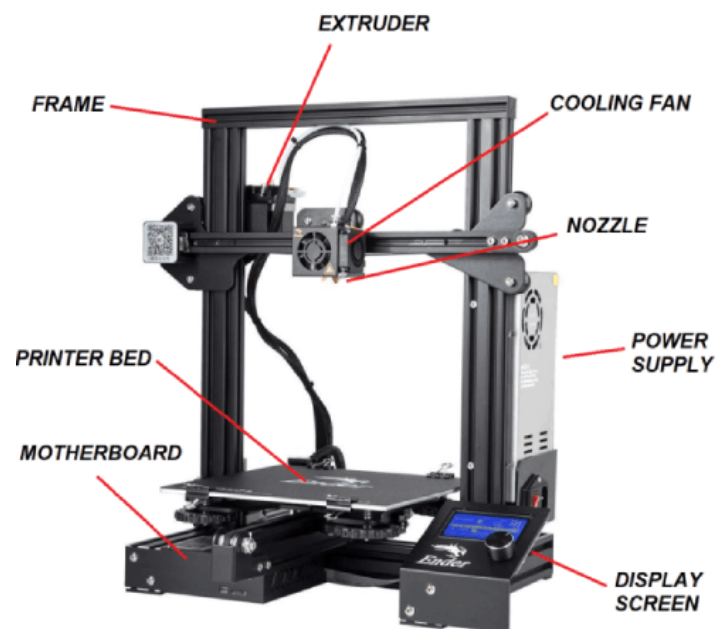


**Figure 2.** Creality Ender 3 V2 FDM 3D Printer.

#### 2.2.2. Autoclave

A machine called an autoclave is frequently used in the medical industry to sterilize and disinfect medical equipment at high temperatures and pressures. Together with the medical sector, Autoclave also offers chemical sector services, including rubber vulcanization,

coating post-treatment, and isothermal synthesis. The pre- or post-processing of composites is a common usage for industrial autoclaves, often known as composite autoclaves [19].

Industrial auto-claves are widely used in a variety of applications, including aerospace and aviation, space and military, Comac, Foker GKN, and many other industries. They work on modern breakthroughs such as electric flying taxis, automobile chassis, and accessories, as well as parts for drones and lightweight weight helicopter components. They also process parts for F1 cars.

The autoclave chamber utilized in this investigation was a bespoke model from Haage Anagram GmbH, Germany, which was created specifically to accommodate polymer processing techniques. This autoclave weighs around 1300 kg and can withstand a maximum pressure of 135 bar and a temperature of 185 °C (including a front lid with a weight of 300 kg). It carefully regulates the pressurization with the aid of intake and output valves. It has a thermocouple heating system that is incorporated directly into the cylinder surface. The autoclave setup in the lab is shown in Figure 3. A sensor was used to detect the pressure and temperature within the autoclave, and the values were shown on the monitor.

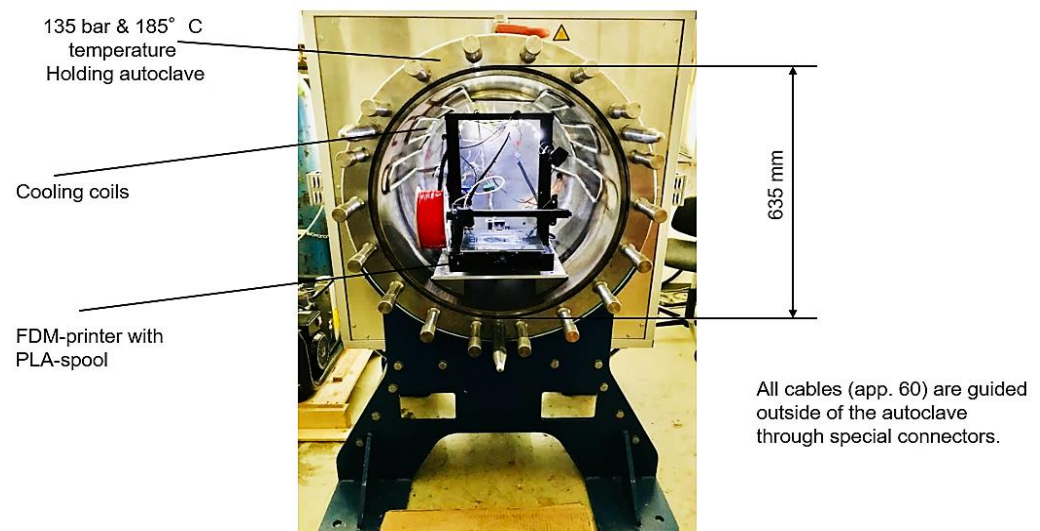


**Figure 3.** 3D Printer setup in the autoclave.

### 2.3. Fabrication of Specimens

#### 2.3.1. 3D Printing

To assess the bonding and consolidation quality of layers, specimens were printed in an autoclave at increased pressure and temperature levels. The testing specimens were created in SolidWorks 2020, in accordance with the testing standards, namely DIN EN ISO 75, which has a rectangular form; and ISO 527 type 1A, which has a dog-bone shape. After designing the component, the file was saved in the STL (standard triangle language) format, as the slicing program can only read STL. By utilizing slicing software to create a G-code that acts as a road map for the extruder to follow in the designated directions, the necessary printing parameters are integrated.

This study made use of a Prusa slicer. The required printing settings are integrated by utilizing slicing software to produce a G-code that serves as a road map for the extruder to follow.

Two orientations were selected for the aligned rectilinear infill pattern, with infill angles of 0° and 90°. This pattern is more suitable for analyzing the mechanical consolidation of layers, since it has more raster lines for better consolidation.

The print speed was 80 mm/min and the layer height was 0.12 mm. This Creality 3D printer required some modification to go inside the autoclave, because it was originally built to function in vacuum and pressure environments. The power supply unit as a whole is linked to the autoclave wall through an integrated connection on the back side.

The unit box of the 3D-control printer was linked outside the autoclave using long wires. On a specially built plate, the 3D printer was put in the autoclave's cylindrical chamber. An infrared night vision camera was installed inside the autoclave to record the video. Significant sections of the 3D printer could not survive high pressure and temperature, because they were not built for such circumstances. The hot-end and electrical capacity of the 3D-motherboard printers were changed to prevent these issues. The autoclave was set to print the test specimens at 0-bar atmospheric pressure, 5-bar compressed air pressure, and 5-bar nitrogen pressure. As the material was PLA, the printing procedure employed a 205 °C nozzle temperature and a 60 °C bed plate temperature. The printing process took place at a temperature of 50 °C inside the autoclave.

A total of 30 samples were produced for testing. Five samples from each test were printed with two distinct printing patterns in an autoclave under two different pressure situations (0 bar, 5 bar in compressed air environment, and, additionally, 5-bar nitrogen atmosphere) (longitudinal and transverse to the pointing direction).

### 2.3.2. Injection Molding

The injection molding process is one of the most common methods for producing large quantities of plastic parts. It is a repetitive process in which melted polymer or plastic is injected into a cavity or cavities, depending on the requirement; packed under pressure; and cooled until the part solidifies [20]. Injection molding is now regarded as one of the most important processes used in the manufacture of plastic products. Injection molding accounts for more than one-third of all thermoplastic materials, and it accounts for more than half of all polymer processing equipment. The main advantage of injection molding is its ability to mass-produce products. The basic principle of injection molding is very straightforward. The plastic material in pellet form is gradually heated until it becomes a viscous melt. The product is then pushed or rammed into a closed mold or cavity that defines its shape [20].

With the same material PLA granules from Herz GmbH, Germany, the injection molding process was performed at temperatures of 50 °C, 110 °C, 120 °C, 155 °C, 180 °C, and 165 °C depending on the different zones present. To produce dog-bone-shaped specimens of the standard ISO 3167 tensile specimen, the 20-s chilling period was maintained. The specimens are manufactured longitudinal. In transverse, the material joins in the middle of the cross-section while along the longer axis in the longitudinal case. The strength of transverse samples seems to be 30% less that of the longitudinal samples, so in all the test results with comparatively better transverse injection-molding samples, strength was considered.

### 2.4. Experimental Setup

The 3D printing was carried out in an autoclave. By using a compressor to introduce compressed air into the autoclave, the pressure was increased inside of it. Using pipelines that were easily accessible in cylinders, a nitrogen gas pressure of 5 bar was established inside the chamber. A 3D printer was combined with an autoclave, as seen in Figure 3.

Heating coils all around the chamber kept it at a constant temperature, and it was completely insulated. At every stage of the experiment, a digital display attached to it displayed the pressure and temperature values in real-time.

### 2.5. Material Tests

#### 2.5.1. Tensile Test

Zwick Proline Z005 tensile testing equipment and Zwick's Test Expert software were used to measure the tensile strength, stiffness, and elongation qualities, in accordance with EN ISO 527.

The strain was measured optically using the VideoXtens-system from Zwick. The basic principle behind a tensile test is to clamp a sample of a material between two fixtures

called “grips.” The length and cross-sectional area of the material are known. The material is then held at one end, while the other is locked and begins to impart weight to it [21].

The equipment holds a piece of material at both ends and gradually pulls it lengthwise until it fractures. The pulling force is termed a load, and it is shown against the length change, or displacement, of the material [22]. The displacement is transformed to a strain value, and the load is transformed into a stress value. A graph of load (weight) against displacement is the result of this test (the amount it stretched). As the amount of weight required to stretch material is dependent on its size (and, of course, its qualities), comparing different materials may be difficult. When designing for structural applications where the material must withstand forces, the ability to make a thorough comparison is critical. Before beginning each test, the external force on the testing machine is kept at zero.

Each printing environment condition was evaluated on a batch of five samples, and the results were averaged to determine the attributes. The external force acting on the testing apparatus should be kept at zero before each test.

#### 2.5.2. Flexural Test

The previously described Zwick-UTM is used in the 3-point bending test, according to DIN EN ISO 178, to characterize the flexural characteristics of materials. The strength or flexural modulus of a material can be assessed using the flexure (bend) test. Lower support span: the material is placed horizontally over two points of contact. Upper loading span: the material is loaded via one or two points of contact until it breaks. The sample’s flexural strength is represented by the highest measured force. Flexure tests do not gauge the basic characteristics of the material, unlike compression or tensile testing. When a specimen is subjected to flexural loading, tensile, compressive, and shear stresses are all present. Hence, a specimen’s flexural characteristics are determined by the combined influence of all three stresses, as well as (to a lesser extent) by the form of the specimen, and the pace at which the load is applied [23].

Flexure tests are the most effective way to assess flexural strength and modulus. The highest stress at the outermost fiber on either the compression or tension side of the specimen is what is referred to as flexural strength. The stress vs. strain deflection curve’s slope is used to compute the flexural modulus. A sample’s endurance of bending or flexure forces can be estimated using these two numbers [23].

#### 2.5.3. Charpy Impact Test

The Charpy impact test (DIN ISO 179) measures impact strength by taking into account how much energy is absorbed by a material when it is exposed to an impacting force. A Ray-Ran pendulum with an impact energy of 4 joules and an impact velocity of 2.9 m/s was used for the impact test [24].

#### 2.5.4. Microscopy Test

The microstructure of a material has an impact on its strength. In this work, a transmitted light microscope was used to examine the damaged surface of 3D-printed PLA samples (Olympus BX40). To prepare the samples for light microscopy analysis, the specimens were broken into small pieces along the damaged surfaces [25].

### 3. Results

#### 3.1. Tensile Test Results

For the injection-molded and 3D-printed samples, the tensile test was conducted at a test speed of 10 mm/min with a grip-to-grip spacing of 115 mm. The linear section of the stress–strain curve was used to compute the Young’s modulus, and the 0.2%-offset technique was used to establish the offset yield strength. The Young’s modulus for all samples is shown in Figure 4.

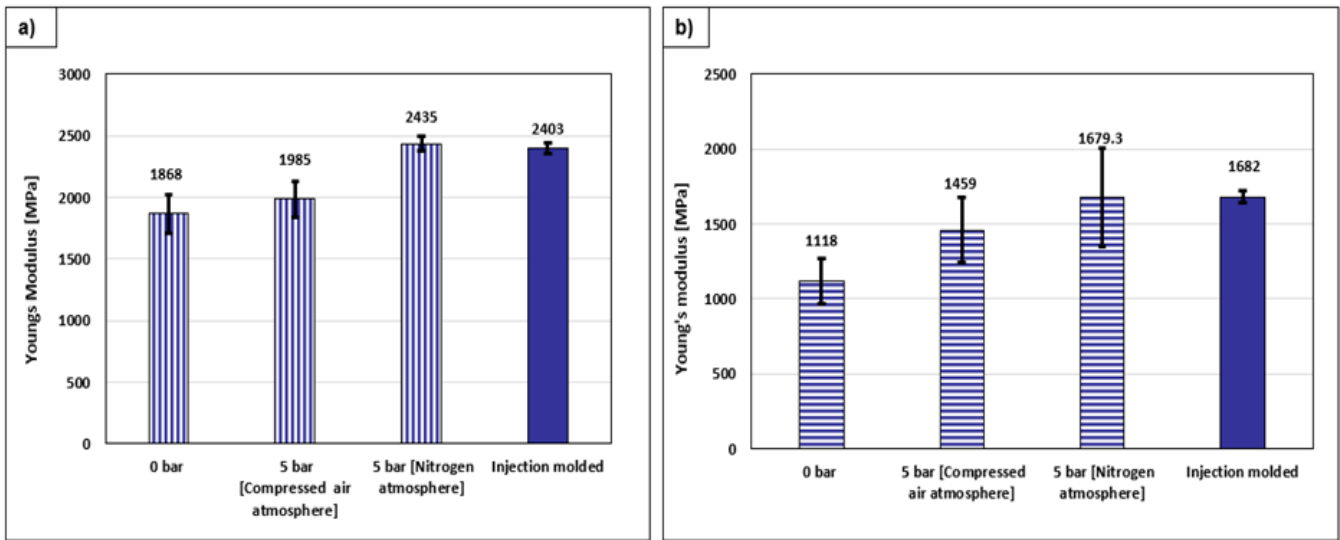


**Figure 4.** Samples printed under various pressure conditions were compared by Young’s modulus longitudinally (a) and transversely (b), with the direction of printing.

Young’s modulus of nitrogen printed samples outperformed the injection-molded ones by a small margin, increasing by 30% in longitudinal and 50.2% in transverse directions. This is according to test results demonstrating how the tensile properties of both longitudinal and transverse samples are affected by a 5-bar nitrogen atmosphere. There are more raster lines in the transverse direction, which allows for better improvement.

Yield strength is a measure of a component’s maximal load-bearing capacity. The longitudinal direction grows by 40.9%, while the transverse direction grows by 47.1%. The yield strain increased by 28% in the longitudinal direction and 11.1% in the transverse direction, as per the secondary scale in Figure 5.

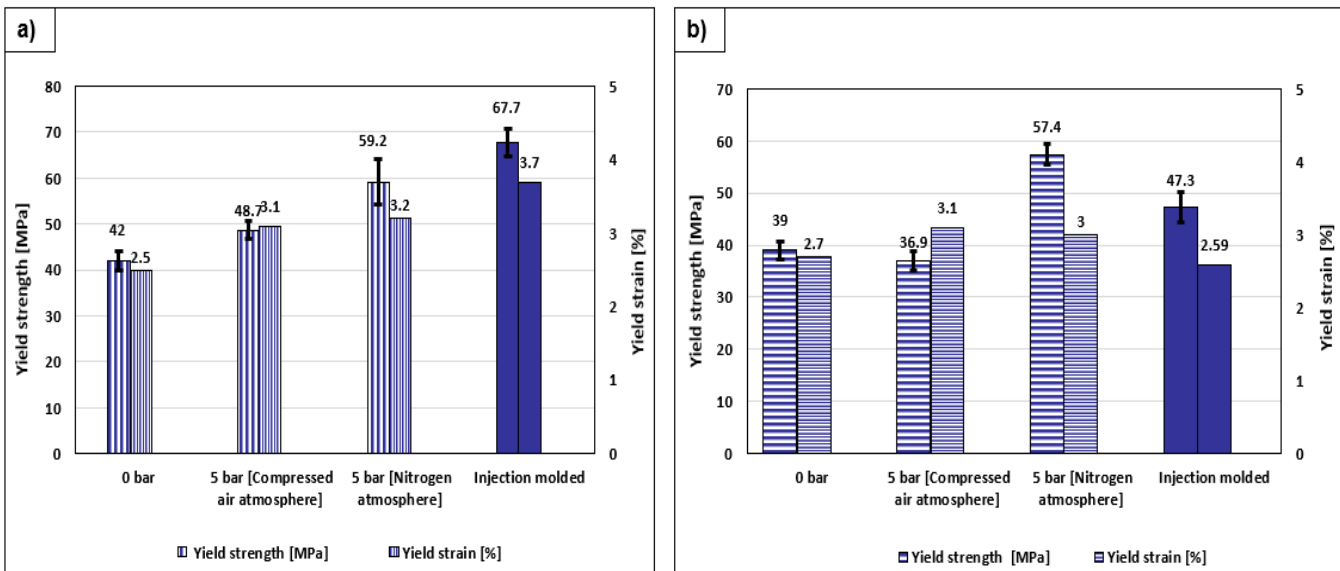
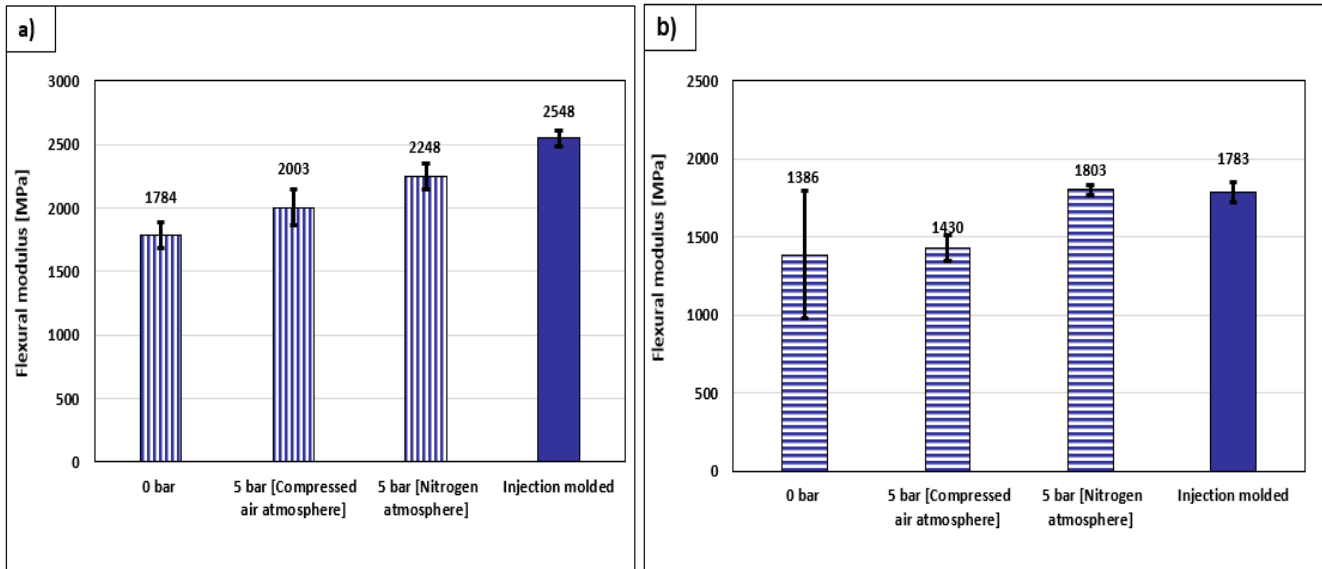


**Figure 5.** Comparison of the yield strength and yield strain of samples printed at various pressure settings longitudinally (a) and transversely (b).

### 3.2. Flexural Tests

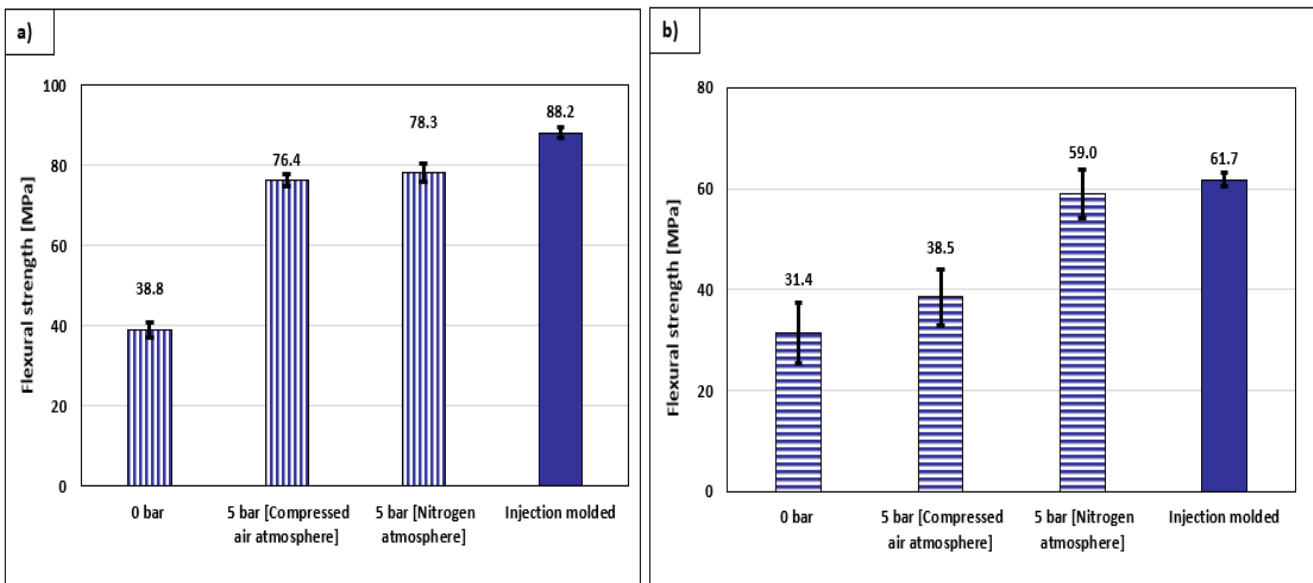
During the flexural test, which made use of the identical Zwick Roell proline, just a small number of the fixtures were changed. The samples used for this test met DIN EN ISO 75 requirements for size (80 × 10 × 4 mm). The test results shown in

Figure 6 show increases in the printed materials' flexural modulus of 26% and 30% in the longitudinal and transverse directions, respectively, in a 5-bar nitrogen environment. The flexural modulus is just 13.3% less and 1% higher in the transverse direction compared to injection-molded samples.



**Figure 6.** Comparison of materials' flexural modulus printed under various pressure levels longitudinally (a) and transversely (b) to the printing direction.

The bending strength of printed samples improved by 101.8% in the longitudinal direction and 87.8% in the transverse direction, according to the comparison of flexural strength in Figure 7. Moreover, samples printed in a nitrogen atmosphere in this instance produced excellent results. When compared to samples that were injection molded, the flexural modulus is only 12.6% less in the longitudinal direction and 4.57% less in the transverse direction.



**Figure 7.** Flexural strength comparison of samples printed under different pressure settings longitudinally (a) and transversely (b).

### 3.3. Charpy Impact Test

In this experiment, Ray-Ran was put through the Charpy impact test with a varied pendulum speed of up to 2.9 m/s. The Charpy impact test, often known as the Charpy V-notch test, is a high strain-rate, standardized exam. The test used in this inquiry was conducted on materials without a notch.

The DIN EN ISO 75 standard used to size the testing specimens ( $80 \times 10 \times 4$  mm). The experiments conducted in a temperature-neutral environment. The pendulum's hammer weighed 951 g. The impact strength comparison is shown in Figure 8. In an autoclave at nitrogen pressure settings ranging from 0 bar to 5 bar, the impact strength of printed samples increased by 73.2% in the longitudinal direction—higher than the injection molded specimens—and 23.6% in the transverse direction. This also implies that nitrogen pressure has a favorable impact on the consolidation layers.

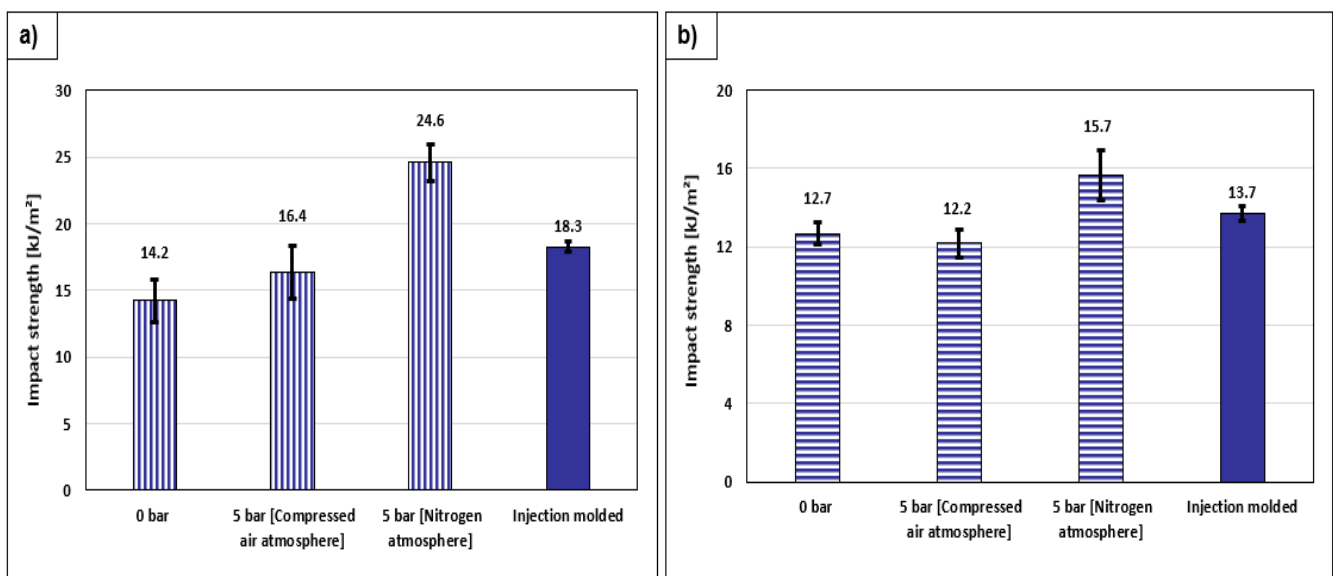


**Figure 8.** Comparison of the impact strength of samples printed under various pressure conditions in the longitudinal (a) and transverse (b) printing directions.

The error bars in every figure represent the average values of the tests that are mentioned throughout, not their precise range. For test specimens, the value variations are not accurate in each scenario. Deviations are unavoidable because 3D printing is such a delicate process, and we placed the setup inside the autoclave.

### 3.4. Microscopy Test Results

The photos below depict a microscopic inspection of test specimens at various pressures. The magnification range employed in this experiment is 200  $\mu\text{m}$ .

Any flaws in 3D-printed components, such as holes, fractures, voids, and air gaps, harm the parts' material qualities. Therefore, in the ultimate finished form of a 3D-printed object, these flaws must be avoided. This study used a transmitted light microscope to investigate samples printed in 0 bar, 5-bar compressed air and 5-bar nitrogen gas atmospheres, and the images are shown in Figures 9–11. The void area is measured in  $\mu\text{m}^2$ , and the voids are designated with various colors. These photos demonstrate how samples produced a string of triangular gaps between two layers along the thickness of the PLA 3D-printed specimens, which exclusively used printed longitudinal examples to aid comprehension.

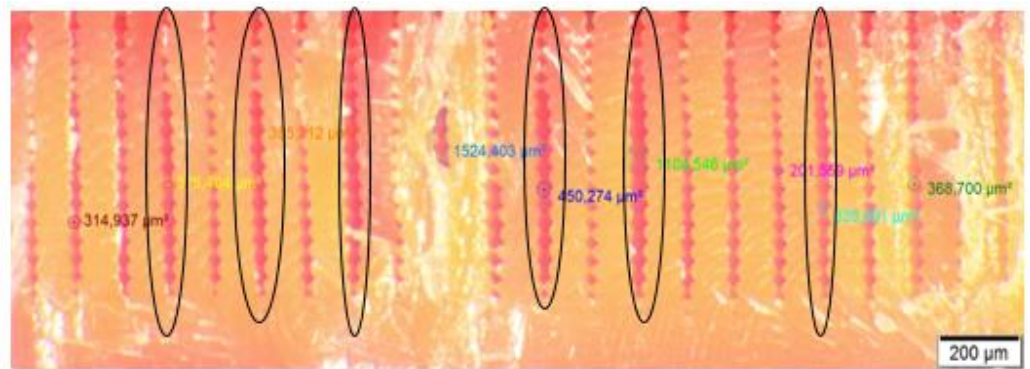


**Figure 9.** The cross-sectional image of a broken FDM 3D-printed specimen in a 0-bar vacuum condition.

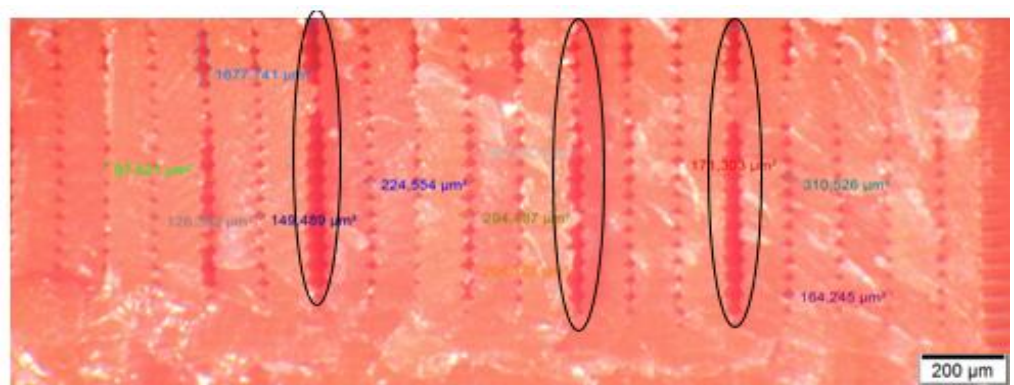


**Figure 10.** The cross-sectional image of a broken FDM 3D-printed specimen in a 5-bar condition.

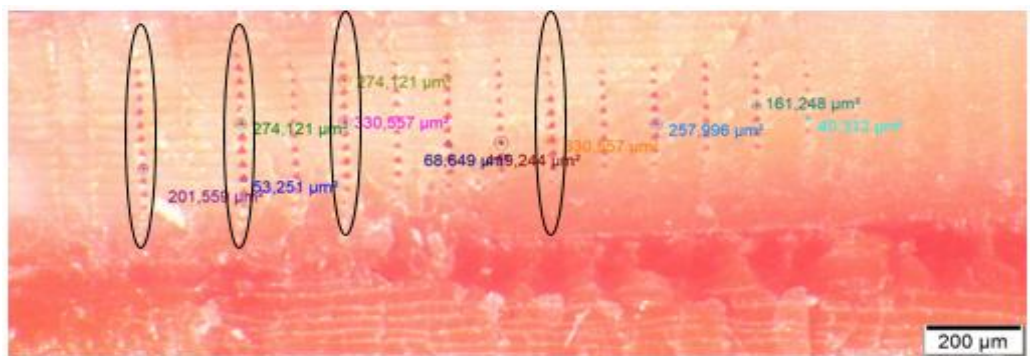


**Figure 11.** The cross-sectional image of a specimen that was broken while being 3D printed using FDM in a 5-bar nitrogen environment.

The results show that samples printed under 0-bar circumstances have more voids, a larger average void area of  $255.51 \mu\text{m}^2$ , and damaged layers. At 5-bar pressure, the average void area was  $141.11 \mu\text{m}^2$ , and void sizes decreased as pressure increased. The voids are significantly smaller in the nitrogen inert gas environment, having been reduced to a minimal level with an average area of  $101.34 \mu\text{m}^2$ —a reduction in the void size of 43%. The empty areas of the injection-molded samples are  $50 \mu\text{m}^2$  or smaller. Table 1 shows the values below.

**Table 1.** Averaged area of voids that were captured during microscopy.

	3D Printing at 0 Bar	3D Printing at 5 Bar	3D Printing At 5 Bar Nitrogen Atmosphere	Injection-Molded Specimen
PLA Voids area ( $\mu\text{m}^2$ )	255.51 $\mu\text{m}^2$	145.11 $\mu\text{m}^2$	101.34 $\mu\text{m}^2$	~50–70 * $\mu\text{m}^2$

Microscopy experiments show that when the pressure in the autoclave grew, the amount of void space decreased to a minimum. The inert gas environment in the chamber will help prevent the oxidation of the printing layers. To corroborate the aforementioned findings, we performed a density test on samples with minimum sizes using the KERN AES-A01 equipment, and we found that there have clearly been decreases in void sizes, which implies that as the void sizes drop, the density would rise. The findings of the density test are listed in Table 2 below. In a nitrogen environment, the PLA 3D-printed materials had a density of 1.1912 gm/cm<sup>3</sup>.

**Table 2.** Results of tests on the density of items created using 3D printing and injection molding under various pressure conditions in the autoclave.

	3D Printing at 0 Bar	3D Printing at 5 Bar	3D Printing At 5 bar Nitrogen Atmosphere	Injection-Molded Specimen
Longitudinal (Average Density)	1.0932 gm/cm <sup>3</sup>	1.1587 gm/cm <sup>3</sup>	1.1912 gm/cm <sup>3</sup>	1.2492 gm/cm <sup>3</sup>
Transverse (Average Density)	1.0462 gm/cm <sup>3</sup>	1.1141 gm/cm <sup>3</sup>	1.1642 gm/cm <sup>3</sup>	1.2492 gm/cm <sup>3</sup>

#### 4. Conclusions

In this work, an autoclave was used to print PLA specimens in two distinct orientations, namely longitudinal and transverse, under three different air conditions. To compare the outcomes, injection molding was also carried out using the same PLA material.

The printing environment is the most crucial element of the 3D-printing process, and has a significant impact on the surface polish, printing quality, and specimen strength. The filament layers may oxidize under normal air circumstances, which may lead to a divergence in the attachment of new layers and would undoubtedly result in larger holes between the layers [8]. In this investigation, the autoclave was kept at 0 pressure and 5 bar of compressed air and nitrogen atmosphere.

The results of all tests show that the samples printed with nitrogen have acquired strength and are nearly equivalent to the strength of injection-molded samples. The samples absorb moisture from the heated compressed air in the autoclave, causing their internal crystalline structure to rearrange, resulting in a bigger grain structure. This aided in the development of modulus and strength. In a nitrogen environment, the young modulus was increased by 30% and 50% in longitudinal and transverse orientations, respectively, and is equal to injection-molded specimens. In both orientations, the yield strength increased by 40% and the flexural modulus by roughly 30%. Flexural strength improved by 100% and 87% in the longitudinal and transverse orientations of printed samples, respectively, and is now very close to injection-molded specimen values. Charpy tests revealed the similar increase in impact strength.

Microscopy and density test results show that 3D-printed materials are more resilient and closely resemble injection-molded samples. The causes for the increased strength of the 3D-printed sample in the autoclave pressure chamber are as follows:

- Autoclave preheating and pressure improved the layer consolidation for 3D printing.

- The nitrogen gas atmosphere in the chamber inhibits layer oxidation, promoting improved layer adhesion.
- A decrease in void size brought on by autoclave pressure

**Author Contributions:** Y.P.S. contributed to data collection, synthesis, and writing of the initial drafts of the manuscript. J.S. helped with research progress and reviewing the report. N.K.N. helped with the analysis of test results. All authors have read and agreed to the published version of the manuscript.

**Funding:** The research work was funded by Hochschule Kaiserslautern-University of Applied Sciences Kaiserslautern, Germany.

**Acknowledgments:** The author would like to thank Jens Schuster for providing laboratory equipment and its facilities at the University of Applied Sciences Kaiserslautern, Germany and IKW.

**Conflicts of Interest:** The authors declare no conflict of interest.

## References

1. Turner, B.N.; Strong, R.; Gold, S.A. A review of melt extrusion additive manufacturing processes: I. Process design and modeling. *Rapid Prototyp. J.* **2014**, *20*, 192–204. [CrossRef]
2. Utela, B.; Storti, D.; Anderson, R.; Ganter, M. A review of process development steps for new material systems in three-dimensional printing (3DP). *J. Manuf. Process.* **2008**, *10*, 96–104. [CrossRef]
3. Wang, X.; Jiang, M.; Zhou, Z.; Gou, J.; Hui, D. 3D printing of polymer matrix composites: A review and perspective. *Compos. Part B Eng.* **2017**, *110*, 442–458. [CrossRef]
4. Kolarevic, B. Digital fabrication: Manufacturing architecture in the information age. In Proceedings of the Association for Computer Aided Design in Architecture, New York, NY, USA, 11–14 October 2001; pp. 268–277.
5. Pucci, U.; Christophe, B.R.; Sisti, J.A.; Connolly, E.S., Jr. Three-dimensional printing: Technologies, applications, and limitations in neurosurgery. *Biotechnol. Adv.* **2017**, *35*, 521–529. [CrossRef] [PubMed]
6. Shaik, Y.P.; Schuster, J.; Katherapalli, H.R.; Shaik, A. 3D Printing under High Ambient Pressures and Improvement of Mechanical Properties of Printed Parts. *J. Compos. Sci.* **2022**, *6*, 16. [CrossRef]
7. Es-Said, O.; Foyos, J.; Noorani, R.; Mendelson, M.; Marloth, R.; Pregger, B. Effect of layer orientation on mechanical properties of rapid prototyped samples. *Mater. Manuf. Process.* **2000**, *15*, 107–122. [CrossRef]
8. Lederle, F.; Meyer, F.; Brunotte, G.P.; Kaldun, C.; Hübner, E.G. Improved mechanical properties of 3D-printed parts by fused deposition modeling processed under the exclusion of oxygen. *Prog. Addit. Manuf.* **2016**, *1*, 3–7. [CrossRef]
9. Yang, C.; Tian, X.; Li, D.; Cao, Y.; Zhao, F.; Shi, C. Influence of thermal processing conditions in 3D printing on the crystallinity and mechanical properties of PEEK material. *J. Mater. Process. Technol.* **2017**, *248*, 1–7. [CrossRef]
10. Shaik, Y.P.; Schuster, J.; Shaik, A.; Mohammed, M.; Katherapalli, H.R. Effect of Autoclave Pressure and Temperature on Consolidation of Layers and Mechanical Properties of Additively Manufactured (FDM) Products with PLA. *J. Manuf. Mater. Process.* **2021**, *5*, 114. [CrossRef]
11. Shaik, Y.P.; Schuster, J.; Chowdary, R. Impact of 3D printing patterns and post-consolidation pressure on mechanical properties of FDM printed samples. *Am. Res. J. Mater. Sci.* **2020**, *1*, 1–10.
12. Robert, J.M.; Ashlie, M.; John, N.; John, S.; Jeff, Y. Cellulose nanomaterials review: Structure, properties, and nanocomposites. *R. Soc. Chem.* **2011**, *40*, 3941–3994.
13. Xionghao, L.; Zhongjin, N.; Shuyang, B.; Baiyang, L. Preparation and mechanical properties of fiber-reinforced PLA for 3D printing materials. IOP conference series. *Mater. Sci. Eng.* **2018**, *322*, 022012.
14. Kiendl, J.; Gao, C. Controlling toughness and strength of FDM 3D-printed PLA components through the raster layup. *Composites Part B* **2020**, *180*, 107562. [CrossRef]
15. Agarwala, M.K.; Jamalabad, V.R.; Langrana, N.A.; Ahmad, S.; Whalen, P.J.; Danforth, S.C. Structural quality of parts processed by fused deposition. *Rapid Prototype J.* **1996**, *2*, 4–19. [CrossRef]
16. Herz GmbH. 20 May 2022. Available online: <https://shop.filamentonline.de/de/38-pla-175mm?> (accessed on 8 February 2022).
17. Upcraft, S.; Fletcher, R. The rapid prototyping technologies. *Assem. Autom.* **2003**, *23*, 318–330. [CrossRef]
18. Creality Ender 3 V2. CREALITY. January 2022. Available online: <https://www.creality3dofficial.eu/products/ender-3-v2-3d-printer?> (accessed on 1 March 2022).
19. Haage Anagramm Technologien GmbH. January 2022. Available online: <https://www.haage.com/DE/produkte/hochdruckautoklaven> (accessed on 1 March 2022).
20. Jürgen, N.; Doreen, S.; Bernd, H.; Matthias, B.; Dieter, P.; Claus, V.; Dieter, L.; Simon, A. Investigations on the formation of composites by injection molding of PA6 and different grafted polypropylenes and their blends. *J. Appl. Polym. Sci.* **2006**, *100*, 2992–2999.
21. Zhou, H. *Computer Modeling for Injection Molding: Simulation, Optimization, and Control*; A John Wiley & Sons. Inc. Publication: Hoboken, NJ, USA, 2013; ISBN 978-0-470-60299-7.

22. Michigan Technology University, Internet Citation (2022) about Tensile Test. Michigan Tech. Available online: <https://www.mtu.edu/materials/k12/experiments/tensile> (accessed on 1 March 2023).
23. Internet Citation (2022) about Flexural Test Resources. Available online: <https://www.testresources.net/applications/test-types/flexural-test> (accessed on 1 March 2023).
24. Tóth, L. Historical background and development of the Charpy test. In *From Charpy to Present Impact Testing*; European Structural Integrity Society: Cassino, Italy, 2002; pp. 3–19.
25. Miao, L.; Dwayne, D.A.; Dongsheng, Z. Displacement/strain measurements using an optical microscope and digital image correlation. *Opt. Eng.* **2006**, *45*, 033605.

**Disclaimer/Publisher's Note:** The statements, opinions and data contained in all publications are solely those of the individual author(s) and contributor(s) and not of MDPI and/or the editor(s). MDPI and/or the editor(s) disclaim responsibility for any injury to people or property resulting from any ideas, methods, instructions or products referred to in the content.